JACS
JOURNAL OF THE AMERICAN CHEMICAL SOCIETY
Communication
pubs.acs.org/JACS

Different Rates of Singlet Fission in Monoclinic versus Orthorhombic Crystal Forms of Diphenylhexatriene

Robert J. Dillon, Geoffrey B. Piland, and Christopher J. Bardeen*

Department of Chemistry University of California, Riverside, California 92521, United States

Supporting Information

ABSTRACT: The dynamics of singlet fission (SF) are studied in monoclinic and orthorhombic crystals of 1,6-diphenyl-1,3,5-hexatriene. Picosecond time-resolved fluorescence measurements and the presence of a strong magnetic field effect indicate that up to 90% of the initially excited singlets undergo SF in both forms. The initial SF and subsequent triplet pair dissociation rates are found to be more rapid in the monoclinic crystal by factors of 1.5 and 3.5, respectively. These results provide clear evidence that molecular organization affects the rates of triplet pair formation and separation, both important parameters for determining the ultimate utility of a SF material.

Singlet fission (SF), in which an excited singlet state on one chromophore splits into a pair of triplet states on different chromophores,[1] is of interest as a way to enhance solar energy conversion efficiencies.[2] One criterion for a useful SF material is that it produces triplets in high yield, which means the singlet→triplet pair reaction should be rapid. It has been proposed that this rate depends critically on the interaction geometry between participating chromophores, and this dependence has been the subject of several theoretical investigations.[3] A second criterion concerns the accessibility of the triplet products. Ideally, the triplet states would have long lifetimes, allowing them to diffuse over long distances, as well as sufficient energy to undergo ionization[4] or energy-transfer reactions. SF has been most thoroughly studied in the polyacenes,[5] which tend to have relatively low energy triplet states.

The observation of efficient SF in carotenoid aggregates[6] suggests that polyene-based molecules may provide an alternative to the polyacenes. In this Communication, we report on the photophysical behavior of crystalline 1,6-diphenyl-1,3,5-hexatriene (DPH), a compound that allows us to address both issues raised in the preceding paragraph. DPH crystallizes into two different polymorphs, a monoclinic form (Figure 1a,b) and an orthorhombic form (Figure 1c,d).[7] This polymorphism can be controlled using different crystallization conditions and provides an opportunity to study how the SF rate depends on molecular arrangement without having to modify the molecular structure. Furthermore, we characterize the triplet dynamics subsequent to the SF reaction to determine which polymorph demonstrates favorable triplet diffusion properties.

In order for SF to take place, it is usually assumed that the excited singlet S* and triplet T_1 energies must fulfill $E(S^*) \geq 2E(T_1)$. In DPH, $E(T_1)$ has been measured to be ~12 400 cm^{-1},[8] but the nature of the S* state is complicated. Figure 2a shows the absorption and fluorescence spectrum for DPH in dilute hexanes solution. Also marked by a red line is $2E(T_1)$. While the absorption is dominated by the strongly allowed $S_0 \rightarrow S_2$ transition, several workers have suggested that the emission originates from a mixture of the S_2 state (^{1}Bu) and the lower

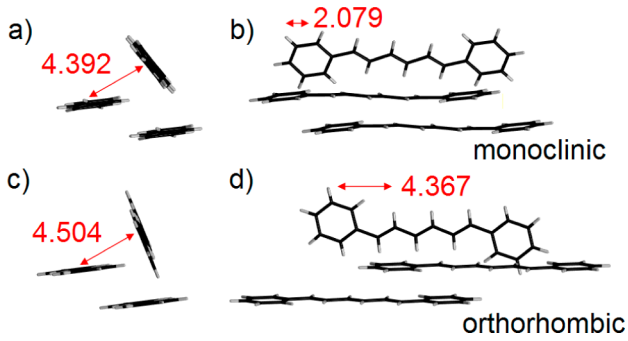

Figure 1. Crystal packing patterns of monoclinic DPH [(a) top-down view and (b) side view] and orthorhombic DPH [(c) top-down view and (d) side view] from ref 7. The edge-to-face distance and vertical slip distance are measured from the long axis of each molecule; all values are in angstroms.

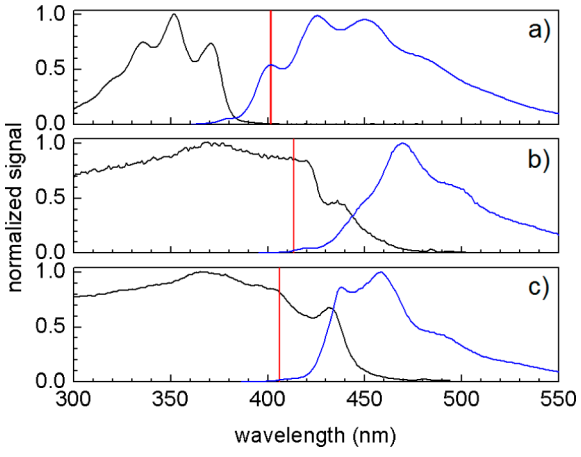

Figure 2. Steady-state spectra of DPH: absorption and fluorescence spectra of monomer in hexanes solution (a), and fluorescence excitation and emission spectra of single crystals of monoclinic (b) and orthorhombic (c) forms. The red line in each plot indicates the $2E(T_1)$ energy.

Received: September 6, 2013
Published: October 30, 2013

   dx.doi.org/10.1021/ja409266s | J. Am. Chem. Soc. 2013, 135, 17278−17281

energy S_1 state (^{1}Ag) that are in rapid equilibrium.[9] In the fluorescence spectrum, the small emission peak at 380 nm is attributed to the S_2 state. We found that the lifetime of this peak mirrors that of the longer wavelength emission peaks (Figure S2), consistent with the idea that either the S_1 and S_2 states are in rapid equilibrium or the emission originates from one state with mixed S_1 and S_2 character. In either case, the equilibrated S* excited-state population resides at an energy higher than the accepted value for $E(S_1)$. If we take the singlet energy to be the mean energy of the lowest energy absorption peak and highest energy emission peak, we obtain $E(S^*)$ = 26 700 cm^{-1}, and $\Delta_{2T\text{-}S} = 2E(T_1) - E(S^*) = -1770$ cm^{-1}. Therefore, SF should be exoergic for isolated DPH molecules.

When the DPH molecules crystallize, both singlet and triplet states shift in energy. Accurate measurement of the absorption and fluorescence spectra of solid-state samples is challenging.[10] For DPH single crystals grown from hexanes solution (monoclinic) and by sublimation under an inert atmosphere (orthorhombic), we measured the fluorescence excitation and emission spectra shown in Figure 2b,c, which are in reasonable agreement with those previously measured for thin films whose crystal structure was not determined.[11] In both crystals, the excitation spectrum exhibits a pronounced low-energy shoulder at 430−440 nm, which we assigned to a defect state (Figure S3). The true $S_0 \rightarrow S_1$ energy is given by the absorption edge to the short-wavelength side of this feature. By fitting the excitation line shape to a set of Gaussians, we obtain $E(S_0 \rightarrow S_1)$ values for the monoclinic and orthorhombic forms (Table 1). While the relative amplitudes of the vibronic peaks in the emission spectra are distorted by self-absorption effects (Figure S4), high-energy emission peaks are observed at 422 nm in the monoclinic and 413 nm in the orthorhombic crystals. As in the monomer, fluorescence lifetime measurements confirm that the high-energy peaks originate from the equilibrated excited-state population (Figure S6) and not impurities or transient intermediates. The high-energy peaks may reflect the mixed S_2 character of the emitting state as in the monomer, but they may also originate from a H-type exciton state.[12] The important point is that identification of the low-energy absorption and highest energy emission peaks allows us to average their energies to estimate E(S*) values, as tabulated in Table 1. Wolf and co-workers measured the delayed fluorescence excitation spectrum to obtain $E(T_1)$ for both crystal forms,[13] and $2E(T_1)$ is shown as a red line in Figure 2b,c.

Table 1. Singlet and Triplet Energies

sample	$S_0 \rightarrow S_1$	$S_1 \rightarrow S_0$	S*	$S_0 \rightarrow T_1$	$\Delta_{2T\text{-}S}$
monomer	26 950	26 390	26 670	12 450	−1 770
monoclinic	23 960	23 720	23 840	12 090	340
orthorhombic	24 390	24 210	24 300	12 310	320

Details of the calculations and references are given in the text. All values are in cm^{-1}. Error range is ±50 cm^{-1}.

The $S_0 \rightarrow S_1$ transition energies shift more than 2000 cm^{-1} on going from solution to the crystal (Table 1), while the triplet-state energies shift by only about 1/10 of this value. This large difference in energetic shifts is expected since the $S_0 \rightarrow T_1$ transition dipole moment is negligible, making this transition much less sensitive to environmental perturbations.[14] From Table 1, we find values of $\Delta_{2T\text{-}S}$ = 340 cm^{-1} for the monoclinic form and 320 cm^{-1} for the orthorhombic form, which are the same to within the experimental error of ±50 cm^{-1}. Due to the large singlet energy shifts, SF becomes slightly endoergic in both crystal forms of DPH, but this does not necessarily preclude rapid SF. An even larger energetic mismatch exists in crystalline tetracene, where the SF reaction proceeds rapidly at room temperature.[15]

Dynamic evidence for the role of SF is obtained by measuring the singlet-state decay using time-dependent fluorescence. Logarithmic plots of the fluorescence decays of the monomer in toluene, along with the monoclinic, and orthorhombic crystal forms, are shown in Figure 3a for a 1 ns time window. In toluene, the decay is single exponential with a time constant of 6.53 ns. In the crystals, the fluorescence decay is strongly non-exponential with an initial decay time on the order of 300 ps in the monoclinic form but slower in the orthorhombic form. The initial fast decay is followed by a longer-lived multiexponential fluorescence decay. We attribute the long-lived decay component to delayed fluorescence from the singlet state re-formed by triplet fusion (TF), based on the fact that the spectrum of the initial component (0−100 ps) is identical to that of later components (Figure S7). In both monoclinic and orthorhombic crystals, the delayed fluorescence decayed with a single-exponential decay time of 50 ± 5 μs, which places a lower limit on the triplet lifetime. The long-lived monoclinic fluorescence decay is shown in Figure 3b. The fluorescence decays were insensitive to preparation conditions: single crystals and ultrathin polycrystalline films grown by solution or vapor deposition show the same initial and delayed fluorescence kinetics (Figure S8).

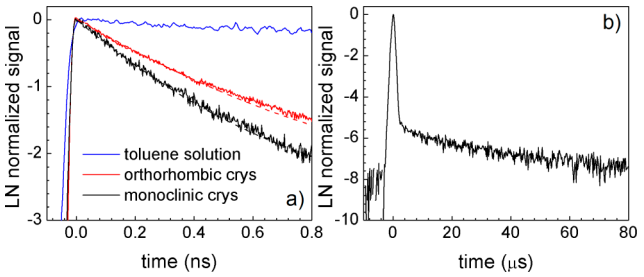

Figure 3. (a) Fluorescence decays in a 1 ns window for DPH in toluene (blue), monoclinic crystal (black), and orthorhombic crystal (red). The dashed lines are the calculated decays using the Merrifield kinetic model with the parameters in Table 2. (b) Decay of the delayed fluorescence of monoclinic DPH in a 100 μs window.

While the presence of a rapid singlet decay channel is consistent with the presence of SF, it is not conclusive proof. One method for assessing whether a singlet decay channel involves triplet products is to look for magnetic field effects on the fluorescence dynamics.[1a,16] If triplet states are involved, magnetic-field-induced changes in their wave functions lead to changes in the singlet↔triplet interconversion rates. In both monoclinic and orthorhombic crystals, the molecules are close to parallel, and application of a magnetic field decreases the number of triplet pair states with singlet character from 3 to 2, out of 9 possible pair states.[17] This decrease in the number of triplet states coupled to the singlet should increase the amount of "prompt" fluorescence after the initial 1 ns decay. Figure 4 shows a clear enhancement of the fluorescence signal in the 20 ns time window for both (a) monoclinic and (b) orthorhombic crystals in the presence of a 8100 G magnetic field. This increase is similar to what has been observed in amorphous rubrene and crystalline tetracene,[17,18] materials in which the

dx.doi.org/10.1021/ja409266s | J. Am. Chem. Soc. 2013, 135, 17278−17281

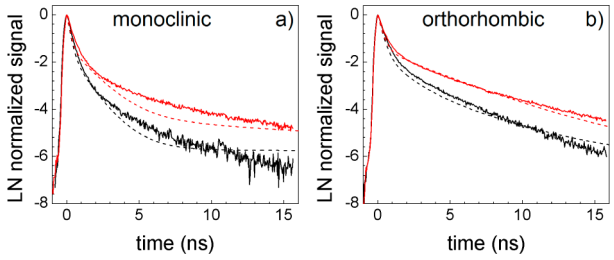

Figure 4. Magnetic field dependence of the fluorescence for the monoclinic crystal (a) and the orthorhombic crystal (b). The black curves are the data with no applied field, and the red curves are in the presences of an 8.1 kG field. Dashed lines are the calculated decays using the Merrifield kinetic model using the parameters in Table 2

singlet decay is dominated by SF. In contrast, the fluorescence decay of DPH molecules dispersed in polystyrene is single exponential and insensitive to magnetic field (Figure S9), as expected when the SF decay channel is not available.

The magnetic field effects can be modeled using a modified Merrifield kinetic model:

$$S^* \underset{k_2|C_s^l|^2}{\overset{k_{-2}|C_s^l|^2}{\rightleftharpoons}} [TT] \underset{k_1}{\overset{k_{-1}}{\rightleftharpoons}} [T\cdots T] \quad (1)$$

where [TT] represents a closely associated triplet pair that can fuse back to the singlet state S*, [T···T] represents spatially separated triplets that cannot directly recombine, and $|C_s^l|^2$ represents the singlet overlap of the lth triplet pair state (out of 9 possible).[17,18] This model describes the low intensity regime where nongeminate recombination is negligible. In order to accurately reproduce the size of the magnetic field effect, we included a magnetic-field-dependent spin−lattice relaxation rate, k_{relax}, that decreases by a factor of 10 at high magnetic fields. Details of the kinetic model are given in the Supporting Information. Simulation of the fluorescence decays yielded the rate constants summarized in Table 2. The fluorescence decays

Table 2. Kinetic Rates Used To Simulate the Crystal Fluorescence Decays

crystal	k_{rad}	k_1	k_{-1}	k_2	k_{-2}	k_{relax}
mono	0.21	0.05	0.7	1.8	3.4	0.5 (0.05)
ortho	0.21	0.01	0.2	1.3	2.3	0.5 (0.05)

The decays were simulated using the kinetic scheme given in eq 1 and the kinetic equations given in the Supporting Information. The values for k_{relax} in parentheses were used to simulate the decays at high magnetic field. All values are in ns^{-1}.

calculated using these parameters are overlaid with the data in Figures 3 and 4. The agreement is quantitative in the 1 ns window, and the calculations do a reasonable job of reproducing the 20 ns data. The kinetic model contains five parameters listed in Table 2, and it is worth considering how sensitive the calculated curves are to the details of the model. The initial decay (<0.5 ns) is determined solely by the k_{-2} fission rate, and thus the different k_{-2} rates in Table 2 are model independent. If we take the lifetime of DPH in the absence of SF to be that of the isolated molecule in polystyrene (0.21 ns^{-1}), we estimate from the k_{-2} values that up to 90% of the initially excited DPH molecules undergo SF. The k_2 fusion rate is fixed by the point where the initial fast decay gives way to a slower delayed fluorescence and should also be robust with respect to model choice. There is more flexibility to adjust the k_1, k_{-1}, and k_{relax} rates to match the longer time delayed fluorescence dynamics in the 20 ns window, so the absolute magnitudes of these rates should be viewed with more caution.

The different k_{-2} rates for the monoclinic and orthorhombic crystals of DPH provide clear evidence that the SF rate depends on molecular organization. The experimental ratio ($k_{-2}^{mono}/k_{-2}^{ortho}$) ≅ 1.5 cannot be explained by the different energetics in the two crystals. An Arrhenius calculation of the ratio of rates gives

$$\frac{k_{-2}^{mono}}{k_{-2}^{ortho}} = \exp\left[-\frac{(\Delta_{2T-S}^{mono} - \Delta_{2T-S}^{ortho})}{kT}\right] \quad (2)$$

Assuming $A^{mono} = A^{ortho}$ and using the values from Table 1, we calculate $k_{-2}^{mono}/k_{-2}^{ortho} = 0.9$ at 298 K. But this calculation should be viewed with caution in light of the uncertainties in the S* and T_1 energies. A shift of 60 cm^{-1} (~1 nm) in the monoclinic S_1 energy would lead to a calculated $k_{-2}^{mono}/k_{-2}^{ortho} = 1.2$, closer to the experimentally observed value. Measuring the fission/fusion rates as a function of temperature would be valuable to precisely determine the barriers for SF in both crystal forms. A second possible explanation is that $A^{mono} \neq A^{ortho}$. Several groups have developed theories to describe SF between neighboring chromophores,[3] and Smith and Michl have proposed an explicit formula for the SF rate that depends on the sum of atomic orbital HOMO/LUMO wave function overlaps of the molecular pair.[19] By symmetry, this sum is zero for perfectly aligned molecules, and the authors have suggested that molecular pairs with a "slip" of 50% provide the ideal geometry for SF. From the structures in Figure 1, both the distance between the π systems and their slip increase in the orthorhombic form. These changes may offset each other: the increased separation would decrease orbital overlap and thus decrease k_{-2}, while the increased slip would increase k_{-2}. From our results, it would appear that the intermolecular separation contribution dominates, leading to a net decrease in the k_{-2} rate for the orthorhombic form. A third factor that could influence the value of k_{-2} is the possible presence of intermolecular excitonic states.[10] If the singlet state is delocalized, the electronic interaction terms that govern k_{-2} may be averaged over multiple DPH molecules, reducing its sensitivity to individual molecular positions. This might explain why the k_{-2} rates are so similar in the two crystal forms.

A second notable difference between the monoclinic and orthorhombic fluorescence decays is the lower overall level of delayed fluorescence for the monoclinic form. The amplitude of the delayed fluorescence is determined by k_1, k_{-1}, and k_{relax}. k_{relax} reflects spin−lattice relaxation, a localized process that is expected to be insensitive to crystal packing. The decrease in k_{relax} in the presence of a magnetic field has previously been observed in SF/TF materials,[20] and can arise through several different physical mechanisms.[21] The k_1 and k_{-1} rates reflect the rate of separation and association of the triplet pairs and should be proportional to the triplet exciton diffusion constant. Both rates are higher in the monoclinic crystal, which likely reflects more rapid exciton hopping. In the orthorhombic form, the larger separation of neighboring DPH molecules is expected to reduce the triplet hopping rate,[22] resulting in smaller observed k_1/k_{-1} values.

In summary, the rapid fluorescence decay and strong magnetic field effect in crystalline DPH indicate that up to 90% of the initially excited singlets undergo SF. Compared to the prototypical SF material tetracene, DPH crystals have the

dx.doi.org/10.1021/ja409266s | J. Am. Chem. Soc. 2013, 135, 17278−17281

advantages of longer triplet lifetimes (≥50 μs) and significantly higher triplet energies (~12 000 cm^{-1}). By taking advantage of crystal polymorphism, we have provided unambiguous evidence that molecular packing affects the rates of SF and triplet pair separation, both important parameters for determining the ultimate utility of a SF material.

■ ASSOCIATED CONTENT

Supporting Information

Sample preparation, experimental details, crystal packing information, spectral fitting, wavelength dependence data, and magnetic field simulation data. This material is available free of charge via the Internet at http://pubs.acs.org.

■ AUTHOR INFORMATION

Corresponding Author

christopher.bardeen@ucr.edu

Notes

The authors declare no competing financial interest.

■ ACKNOWLEDGMENTS

This work was supported by the National Science Foundation under grant CHE-1152677. G.B.P. acknowledges support through a U.S. Department of Education GAANN Award, P200A120170.

■ REFERENCES

(1) (a) Swenberg, C. E.; Geacintov, N. E., Excitonic interactions in organic solids. In *Organic Molecular Photophysics*; Birks, J. B., Ed. Wiley & Sons: Bristol, 1973; Vol. *1*, pp 489−564; (b) Smit;h, M. B.; Michl, J. *Chem. Rev.* **2010**, *110*, 6891−6936.

(2) (a) Hanna, M. C.; Nozik, A. J. *J. Appl. Phys.* **2006**, *100*, 074510/1−074510/8. (b) Congreve, D. N.; Lee, J.; Thompson, N. J.; Hontz, E.; Yost, S. R.; Reusswig, P. D.; Bahlke, M. E.; Reineke, S.; Voorhis, T. V.; Baldo, M. A. *Science* **2013**, *340*, 334−337.

(3) (a) Beljonne, D.; Yamagata, H.; Bredas, J. L.; Spano, F. C.; Olivier, Y. *Phys. Rev. Lett.* **2013**, *110*, 226402/1−226402/5. (b) Berkelbach, T. C.; Hybertsen, M. S.; Reichman, D. R. *J. Chem. Phys.* **2013**, *138*, 114102/1−114102/16. (c) Greyson, E. C.; Stepp, B. R.; Chen, X.; Schwerin, A. F.; Paci, I.; Smith, M. B.; Akdag, A.; Johnson, J. C.; Nozik, A. J.; Michl, J.; Ratner, M. A. *J. Phys. Chem. B* **2010**, *114*, 14223−14232. (d) Zimmerman, P. M.; Musgrave, C. B.; Head-Gordon, M. *Acc. Chem. Res.* **2013**, *46*, 1339−1347. (e) Johnson, J. C.; Nozik, A. J.; Michl, J. *Acc. Chem. Res.* **2013**, *46*, 1290−1299.

(4) Aryanpour, K.; Munoz, J. A.; Mazumdar, S. *J. Phys. Chem. C* **2013**, *117*, 4971−4979.

(5) (a) Wilson, M. W. B.; Rao, A.; Ehrler, B.; Friend, R. H. *Acc. Chem. Res.* **2013**, *46*, 1330−1338. (b) Ramanan, C.; Smeigh, A. L.; Anthony, J. E.; Marks, T. J.; Wasielewski, M. R. *J. Am. Chem. Soc.* **2012**, *134*, 386−397. (c) Roberts, S. T.; McAnally, E. R.; Mastron, J. N.; Webber, D. H.; Whited, M. T.; Brutchey, R. L.; Thompson, M. E.; Bradforth, S. E. *J. Am. Chem. Soc.* **2012**, *134*, 6388−6400. (d) Chan, W.-L.; Berkelbach, T. C.; Provorse, M. R.; Monahan, N. R.; Tritsch, J. R.; Hybertsen, M. S.; Reichman, D. R.; Gao, J.; Zhu, X.-Y. *Acc. Chem. Res.* **2013**, *46*, 1321−1329.

(6) Wang, C.; Tauber, M. J. *J. Am. Chem. Soc.* **2010**, *132*, 13988−13991.

(7) Harada, J.; Harakawa, M.; Ogawa, K. *CrystEngComm* **2008**, *10*, 1777−1781.

(8) (a) Bensasson, R.; Land, E. J.; Lafferty, J.; Sinclair, R. S.; Truscott, T. G. *Chem. Phys. Lett.* **1976**, *41*, 333−335. (b) Ramamurthy, V.; Caspar, J. V.; Corbin, D. R.; Schlyer, B. D.; Maki, A. H. *J. Phys. Chem.* **1990**, *94*, 3391−3393.

(9) (a) Itoh, T.; Kohler, B. E. *J. Phys. Chem.* **1987**, *91*, 1760−1764. (b) Bachilo, S. M.; Spangler, C. W.; Gillbro, T. *Chem. Phys. Lett.* **1998**, *283*, 235−242. (c) Kupper, B.; Kleinschmidt, M.; Schaper, K.; Marian, C. M. *ChemPhysChem* **2011**, *12*, 1872−1879.

(10) Bardeen, C. J. *MRS Bull.* **2013**, *38*, 65−71.

(11) Sonoda, Y.; Kawanishi, Y.; Ikeda, T.; Goto, M.; Hayashi, S.; Yoshida, Y.; Tanigaki, N.; Yase, K. *J. Phys. Chem. B* **2003**, *107*, 3376−3383.

(12) Spano, F. C. *Acc. Chem. Res.* **2010**, *43*, 429−439.

(13) Weiss, W.; Port, H.; Wolf, H. C. *Chem. Phys. Lett.* **1992**, *192*, 289−293.

(14) Andrews, J. R.; Hudson, B. S. *J. Chem. Phys.* **1978**, *68*, 4587−4593.

(15) (a) Chan, W. L.; Ligges, M.; Zhu, X. Y. *Nat. Chem.* **2012**, *4*, 840−845. (b) Burdett, J. J.; Gosztola, D.; Bardeen, C. J. *J. Chem. Phys.* **2011**, *135*, 214508/1−214508/10.

(16) Geacintov, N.; Pope, M.; Vogel, F. *Phys. Rev. Lett.* **1969**, *22*, 593−596.

(17) Piland, G. B.; Burdett, J. J.; Kurunthu, D.; Bardeen, C. J. *J. Phys. Chem. C* **2013**, *117*, 1224−1236.

(18) Burdett, J. J.; Piland, G. B.; Bardeen, C. J. *Chem. Phys. Lett.* **2013**, *585*, 1−10.

(19) Smith, M. B.; Michl, J. *Annu. Rev. Phys. Chem.* **2013**, *64*, 361−386.

(20) (a) Funfschilling, J.; Altwegg, L.; Zschokke-Granacher, I.; Chabr, M.; Williams, D. F. *J. Chem. Phys.* **1979**, *70*, 4622−4625. (b) Altwegg, L. *Chem. Phys. Lett.* **1979**, *63*, 97−99.

(21) Tarasov, V. V.; Zoriniants, G. E.; Shushin, A. I.; Triebel, M. M. *Chem. Phys. Lett.* **1997**, *267*, 58−64.

(22) You, Z.-Q.; Hsu, C.-P.; Fleming, G. R. *J. Chem. Phys.* **2006**, *124*, 044506/1−044506/10.